Journal of Achievements in Materials and Manufacturing Engineering
VOLUME 23
ISSUE 1
July
2007

Finite element analysis of the interaction between an AWJ particle and a polycrystalline alumina ceramic

P. Gudimetla*, P.K.D.V. Yarlagadda
School of Engineering Systems, Queensland University of Technology,
Gardens Point Campus, 2 George Street, Brisbane Q4001, Australia
* Corresponding author: E-mail address: p.gudimetla@qut.edu.au

Received 16.04.2007; published in revised form 01.07.2007

Analysis and modelling

ABSTRACT

Purpose: Abrasive waterjet cutting involves use of a high pressure, abrasive laden waterjet at trans-sonic speeds to cut difficult-to-machine materials. The jet-material interaction depends on the nature of the material being cut, such as ductile or brittle. The brittle regime involves the generation and propagation of microcracks due to impact and many theories have been proposed in this regard. We aim to resolve the nature of the generation and propagation of cracks in such phenomena using the finite element analysis methodology.
Design/methodology/approach: A 3-dimensional FE model was set up using PATRAN. The alumina ceramic was modelled as a 1-mm cube while a 0.1mm diameter half sphere was used to model a single abrasive particle. The system was imported into ABAQUS and an explicit analysis was performed. The element deletion method was used after invoking a failure criterion to estimate the number of elements removed due to a single impact. The aggregate volume of eroded material was then calculated by multiplying the number of elements removed with the volume of each element. The results of the FEA were compared with the brittle model proposed by Kim & Zeng [12].
Findings: The results of the FEA indicate that mixed-mode failure is the most common form of failure in such interactions. The volume of material removed per impact from the FE results is close to 16% of those predicted by Kim & Zeng's model.
Research limitations/implications: The finite element framework presented is idealized for the case of regular cubes based on a set of assumptions.
Originality/value: This finite element approach is a good tool to study the nature of interaction between a microscopic particle and a brittle material and accurately predict the erosion mechanisms in such interactions.
Keywords: Numerical techniques; Abrasive waterjet machining; Brittle fracture model; Erosion; ABAQUS

1. Introduction

The abrasive waterjet has been widely used as a high precision cutting tool to process difficult-to-machine and high performance materials such as ceramics and ceramic composites over the decades. The cutting action involves the erosive action of an abrasive laden waterjet at transonic speeds, with the erosion processes well described for both ductile and brittle regimes [1-4]. It is a very valuable tool for a number of applications such as linear and profile cutting and drilling and has proved to be a suitable replacement for laser or plasma cutting systems where there is a need to eliminate a heat-affected zone and to eliminate the residual stresses adjacent to the cutting front (kerf). Apart from cutting, the technique is now also being employed as a surface cleaning system and in controlled destruction of various types [4].

Erosion of ceramic materials in abrasive waterjet cutting is a continuous *dynamic brittle fracture process*. This view is based on the theory that material removal occurs due to the nucleation and proliferation of a network of micro-cracks which intermingle and coalesce to for a microchip of material which is disintegrated from the parent material. The high energy particulate impact creates a localized plastic zone at the particle material interface which plays a crucial role in the micro-cracking process. The damage created on brittle surfaces by quasi-static solid particulate contact has been extensively studied using both the elastic and elastic/plastic indentation regimes [5-8]. In the elastic regime, the maximum tensile stresses are found to be radial, creating circumferential cracks. These cracks are initiated at the surface and propagate inward. In the elastic/plastic regime, the maximum tensile stresses near the surface are tangential and produce radial cracks that propagate outward along the surface, while in the sub-surface, the maximum tensile stresses are approximately parallel to the surface. The formation of circumferential cracks is determined by the flaw properties of the test material as determined by the fracture toughness K_{IC} and the surface flaw distribution. The quasi-static indentation characteristics have been utilized to evaluate such important phenomena as abrasive wear and low-velocity erosion. However, the equally important dynamic erosion phenomenon cannot be regarded as a simple extension of the quasi-static indentation process. This is due to the fact that the material properties are subjected to substantial changes intrinsically, and these may trigger a change in the material's response to drastic dynamic loading and unloading. In this sense, the dynamic properties, such as dynamic hardness for example, that relate to projectile impact are not well understood.

AWJ cutting involves a multivariate process parameter control such as water pressure, abrasive flow rate, jet incidence angle, water flow rate [4]. The finite element approach can be used as an effective tool to optimize the cutting parameters for a variety of materials (both ductile and brittle) using various elasto-plastic and brittle failure models. Further, many useful insights can be gathered with regard to the high velocity particle interaction with the target surface. In this paper, we present a brittle cracking model which uses the dynamic yield criteria to simulate the AWJ erosion of polycrystalline alumina ceramics. The results of the FE models are compared and validated with our own erosion experiments and the predictions of Kim & Zeng's brittle erosion model for ceramics.

2. Microstructural aspects of dynamic failure

The term dynamic failure is used to distinguish certain special characteristics of failure of materials subjected to dynamic loading. The major feature that differentiates dynamic failure from quasi-static failure or behaviour is the presence of stress waves. Stress waves arise due to the applied dynamic load or due to the stresses released from a crack tip at fracture. Abrasive waterjet interaction with a brittle material is a good example of the different phenomena associated with the dynamic failure response of a material. Dynamic (high-velocity) crack propagation has unique aspects that differentiate it from quasi-static fracture including [9]:

- **Rapid crack propagation:** The velocity of the crack can approach the induced shock wave velocity; the Rayleigh wave velocity is widely accepted as the limiting velocity, but this is rarely achieved in materials, where the maximum values are closer to 1000 m/s. At sufficiently high velocity, there is a tendency for cracks to bifurcate, thereby lowering the overall energy of the system. Thus, quasi-static failure tends to produce one large crack while dynamic failure produces many small fragments.
- **Fast Nucleation, growth and coalescence of voids:** The rapid rate of loading makes the independent nucleation and growth of micro-voids possible. The crack will accelerate even further by the lowering of the toughness: brittle toughness is generally less than ductile toughness.
- **Shear band formation:** Localization of plastic deformation in a narrow region takes place when thermal softening is more pronounced than the strain and strain-rate hardening combined. The adiabaticity, or quasi-adiabaticity of the process due to the high strain-rate deformation enhances the propensity for this response. Shear bands are macroscopic, non-crystallographic regions where plastic deformation in a material is highly concentrated. The formation of these shear bands is extremely important in dynamic deformation of materials as they are often precursors to fracture. At low strain rates and moderate levels of strain, slip and twinning are the most common deformation mechanisms in most metals and alloys. Pressure-induced phase transformations can also play an important role in altering the material response. In many materials, as the strain rate increases due to the increasing impact velocity, the local temperature increases due to the heat generated from the deformation accumulation. This, in turn, may lead to a localised deformation to a narrow portion of the sample. This phenomenon is commonly known as shear banding. It is believed that shear banding plays an important role in dynamic fragmentation and fracture process.

2.1. Energy dissipation due to high-velocity impacts

It is apparant that the high velocity impact of a projectile with a solid target results in an extremely complex phenomenon. A complete description of this behaviour would involve consideration from all phases of continuum mechanics theory. In the initial high-pressure phases of the impact, the material behaves essentially as an inviscid, compressible fluid since the pressures are high with respect to the maximum shear stresses that can be developed within the material. A crater is formed that expands rapidly for a time and a shock wave emanates from its surface. A state of plastic deformation follows that apparently decays rapidly into a spherical elastic wave through the target. The many phases involved in the complete description of this contact mechanism further include melting and resolidification, vaporisation and condensation and the kinetics of phase change.

The contact between the projectile and the target is of primary importance in determining the mode and the extent of the damage imparted in the material. The crucial contact parameters are the contact pressure, contact radius and the contact time. Contact pressure determines whether the target response will be elastic or

plastic while the contact radius relates the pressure to the effective applied force F. And the contact time determines the force history, $F(t)$. This force history ultimately establishes the extent of the impact damage, for a specified contact condition, as it directly determines the magnitude of the dynamic stresses outside the contact zone. The damage zone and the crack extension that result from transient elastic stresses should thus depend inversely on the longitudinal wave speed in the target. This may account for the approximate inverse correlation of the raindrop damage in brittle materials within the target hardness because the hardness in such materials tends to scale with the elastic modulus and hence with wave velocity. Also of significance is the flaw formation stress and the fracture toughness. The contact parameters, notably the interface pressure and particle velocity affect the extent of local damage. For plastic target response, there are no equivalent analytic solutions that could provide a similar rationale for damage characterisation.

An estimate of the energy absorbed by elastic waves during the elastic normal impact and rebound of a sphere on a plane target has been given by Hunter [10]. He calculated the energy contained in elastic waves generated by a transient localised normal force on the free surface in terms of the Fourier components of the force, and applied his result to the purely elastic (Hertzian) collision of a sphere with a semi-infinite isotropic body. Hunter showed that the fraction λ of the initial kinetic energy of the sphere that is dissipated as elastic waves as,

$$\lambda \cong 1.27\left(V/C_0\right)^{3/5} \tag{1}$$

In order to estimate the energy absorbed in elastic waves, the force-time relationship for the complete loading and unloading cycle is essential. While the model of ideal plasticity provides a fair estimate of the force history during the loading cycle, it predicts that the force should drop instantaneously to zero as the impacting particle comes to rest. The force history during this unloading period is implicit in Hertz's equations but an explicit analytical expression cannot be obtained. Hunter demonstrated that the numerical solution of the equations can be closely approximated given by the relationship,

$$F_e = F_0 \cos \omega_e (t - \pi/2\omega_p) \tag{2}$$

so that, if the total transient force is $F(t)$, then the total energy W dissipated in elastic waves in the brittle solid is,

$$W = \frac{8\beta(1+\nu)}{\rho_0 C_0^{\,3}} \left(\frac{1-\nu^2}{1-2\nu}\right)^{1/2} F_0^{\,2} \omega_0 \alpha \tag{3}$$

Using the above relations, the fraction of the original kinetic energy of a rigid spherical projectile can be given as,

$$\lambda = \alpha\beta \frac{(1+\nu)}{(1+e)} \left(\frac{1-\nu^2}{1-2\nu}\right)^{1/2} \frac{4\pi\sqrt{6}}{C_0^{\,3}} \frac{\rho}{\rho_0} \left(\frac{P}{\rho}\right)^{3/2} \tag{4}$$

Equation (4) assumes that there is some plastic deformation in the target so that the force-time history can be represented as a case of plastic loading and elastic unloading.

2.2. Brittle erosion of ceramics by abrasive waterjet cutting

In abrasive waterjet machining, the supersonic water stream, laden with abrasives, forms an extremely erosive tool that erodes the target material at a very high rate, forming a kerf. Due to the energy dissipation, the cutting power of the jet decreases along its path (depth of cut) and generates a series of steps at the bottom of the kerf [3]. These steps are believed to lead to large angle impacts. However, the location of the steps implies that they are subject to the impact of the jet deflected by the upper sections of the material and therefore, the impact occurs at glancing angles. Due to the difference in the cutting power of the direct jet and the deflected jet, it is believed that steps are initiated immediately behind the directly impacted zone, as a result of the sudden change of the material removal rate. This phenomenon strongly suggests the existence of a mechanism in which discrete fractures occur simultaneously in the vicinity of the impact site. These discrete fractures may eventually coalesce to forms a crack network resulting in material removal.

The impact erosion of thick ceramics includes two components of material removal. The first is caused by plastic flow at the immediate impact site. The material removal component due to plastic flow can be evaluated with the existing ductile erosion models. The other component of material removal is due to network cracking caused by the impact-induced stress waves. At the site of impact, elastic half space theory [9] predicts the generation of three elastic waves, the P-wave (dilatational wave), S-wave (shear wave) and the surface R-wave (Rayleigh wave). These waves propagate radially outward. When these waves pass a specific zone in the target material, the incompatibility of the local particle motion and the surrounding region will create a complicated stress pattern in the localised zone. From the zone of impact, the original compressive pulse rapidly develops into a negative tensile stress for the sake of divergent propagation. The existence of tensile and shear stresses implicates the destructiveness of these waves associated with impact loading.

At the point of impact, the damage pattern consists of a large number of minute hair-like cracks radiating outward. These cracks are believed to be the result of the tangential stresses created by the propagating spherical compression pulse. The alumina specimen impacted by the abrasive particle at a speed of about 600 m/s is analogous to the fracture damage of a large block of material, caused by detonation charge. The localisation of the damage can be attributed to the wave divergence phenomenon. As the wave propagates outward, it encounters an increasing volume of material and therefore, the energy density will decrease as the travel distance increases (geometric dampling law). Due to the effect of this damping, the destructiveness of these waves will be limited in a small zone around the source, the size of which will depend on the critical fracture energy of the material as well as the input energy of the source.

The fractures produced by the explosive condition are different from those produced by static stresses since the stress duration is so short that any cracks formed do not have the time to propagate. Instead of running cracks, a large number of separate, individual fractures occur and coalesce to form a continuous but irregular fracture surface. A high velocity impact event produces a

pulse of longer duration than explosion but much shorter than a quasi-static condition. Therefore, it is reasonable to assume that the surface craters on the specimen are created by the stress wave during impact. Further, since the atomic bonds in a crystalline material are weaker for atoms located at the grain boundaries, fractures occur on the grain boundaries within a roughly hemispherical zone of certain size and coalesce into a fracture network. This can be accounted for by the granular appearance of the craters.

The material removal component due to network cracking in abrasive waterjet cutting is evaluated with a crack network model [11,12]. The crack network model uses the energy approach, which relates the fracture surface energy in forming the crack network to the stress wave energy transmitted into the target material upon the particle impact. By modifying an expression of the stress wave energy derived by Hutchings [13], this model has successfully predicted the erosion rates of different alumina ceramics under normal impact of an abrasive contained in an abrasive waterjet. The simplified cutting equation is given as,

$$\frac{W}{\left(mv_0/2\right)^2} = \lambda = f_e \eta(\nu)\left(\frac{\rho}{\rho_p}\right)^{1/2}\left(\frac{P}{E}\right)^{3/2} \tag{5}$$

The total energy absorbed by the target during impact can be expressed in terms of the plastic deformation, stress wave energy and residual strain energy. The plastic deformation energy is transmitted through the target material and is dissipated by fractures and internal friction. The residual energy is the balance of the total input energy. It is partially dissipated by fragmentation of the particle and the remaining energy becomes the kinetic energy of the rebounding particle or particle fragments.

According to the crack network model, the stress wave energy is disspated in two modes, fracture and internal friction. It is assumed that that a constant fraction f_w of the stress wave energy is converted into the fracture energy in the process of forming the surrounding crack network. A further assumption is that the surrounding crack network is formed by separate fractures along the grain boundaries within an approximately hemispherical region. Under these conditions, the simplified equation of the fractured volume due to single particle impact is given as,

$$V_f = \frac{f_e f_w a \eta(\nu) m v_0^{\,2} \sin\theta^2}{12\gamma(1-p)}\left(\frac{\rho}{\rho_p}\right)^{1/2}\left(\frac{P}{E}\right)^{3/2} \tag{6}$$

Zeng & Kim's study [10] using scanning electron microscopy (SEM) revealed that the most pronounced impact damage mechanism observed in ceramic materials such as AD 99.5 is intergranular cracking. While transgranular cracking occurs in some individual grains, intergranular cracking mechanism is clearly dominant. Plastic flow and melting occur at the immediate impact site. They experimentally proved that pure waterjets provide minimal erosion of high strength ceramics. However, water plays an important role in flushing away the fractured materials and there is conclusive proof that AWJ cutting is the result of abrasive particle impact at glancing angles and that in most brittle materials, including thick ceramics, the dominant erosion mechanisms constitute intergranular cracking and plastic flow.

Typically, ceramics have much higher resistance to plastic deformation than most metals due to the very high values of hardness and fracture toughness. However, in the event of high velocity impact, the localized stresses at the impact site are so high that even a ceramic can exhibit certain degree of plasticity. Further, the heat generated from this initial plastic deformation is confined to the local zone because of the very high strain rate and poor conductivity of ceramics. This localized heating produces a softening or even melting effect and encourages additional plastic flow.

2.3. Approach to modelling

Computational models for impact damage, dynamic fracture and fragmentation are available in the literature. For most part, these models are based on continuum damage theories, wherein, the net effect of fracture is idealised as a degradation of the elasticity of the material [13]. Additionally fragmentation has often been modelled by recourse to local/global energy balance concepts [14]. It is now an acknowledged fact that continuum theories of fracture and fragmentation suffer from obvious shortcomings. For example, the discrete nature of cracks is lost in the continuum theory. This is abetted by the fact that homogeneizing a cracked solid calls for assumptions regarding the distribution and geometry of the cracks themselves. Further, the determination of the effective properties of a cracked solid under dynamic loading conditions presents additional difficulties that stem from issues as wave propagation along a primary crack and/or secondary cracks [15]. Perhaps, the most fundamental objection to the adoption of continuum theories is that the failure of a brittle specimen is governed by the growth of a single dominant crack. Such a condition is not amenable to homogenization. In this sense, there are very few efforts that have tried to depart from continuum theories and investigated the feasibility of accounting explicitly for individual cracks, as they nucleate, propagate, coalesce and eventually intersect to form a material fragment. In these cases, either the mesh was dense enough to provide 'probable' fracture paths or new surfaces were adaptively created based on cohesive modelling laws. A cohesive law for a particular model is defined as the basis that is used to create a new surface by allowing initially coherent element boundaries to open. The cohesive law determines the work of separation, or fracture energy, required for the complete formation of a new free surface. The modelling approach we have adopted was based more on continuum theory, in the sense that we are interested in finding out the amount of material that can be eroded (the number of elements that can be deleted, in terms of the mesh) by an impacting particle (rigid body). The basis for this is as follows: Under high-velocity impacts, profuse cracking may occur. This can generate many fractures in the vicinity of impact that can intersect to form discrete fragments of dislocated elements within the mesh. If the extent of fragmentation is adequately severe, the comminuted phase will exhibit a certain degree of plasticity. In reality, the material would exhibit granular flow conditions due to localised plasticity. Under these circumstances, the multiple collisions and frictional interactions between the various fragments have to be monitored very

efficiently. In particular, the large number of simultaneous interactions and contact zones demand a contact algorithm for computational efficiency.

To overcome this complication, we have used suitable failure criteria based on the compressive strength of the material. The failure criteria implies that once an element acquires the user-defined compressive stress, it is assumed to have attained the required amount of fracture energy (similar to a cohesive law) to be dislocated from the mesh. This modelling approach was validated and calibrated using a 2-D axi-symmetrical model, for the case of shear failure (using plasticity) and brittle failure. Adaptive meshing was employed in the case axi-symmetric modelling only, while fixed mass scaling approach was used in the case of 3-dimensional modelling. The reason for this is the type of elements used for 3-dimensional modelling do not accommodate for adaptive meshing. So, the recourse was to maintain the values of ratio of deformation speed to wave speed less than one, this being the convergence criterion for all simulations.

The high rate dynamic loading of a body usually results in localised plastic deformations and temperature rises. A significant amount of the plastic work is converted into heat, which is also generated at frictional contacts. The mechanical and thermal equations can be fully coupled as a consequence of thermal softening. Similarly, damage and plasticity can be coupled, as the existence of microcracks introduces local stress concentrations that may induce further plastic deformation.

2.4. Governing equations of motion

Consider a body initially occupying a reference configuration B_0 and a process of incremental loading whereby, the deformation mapping over B_0 changes from ϕ_n, at a time t_n to $\phi_{n+1} = \phi_n + u$ at time $t_{n+1} = t_n + \Delta t$. Dynamic equilibrium is enforced at time t_{n+1} by the virtual work principle,

$$\int_{B_0} P_{n+1} : \nabla_0 \eta dV_0 - \int_{B_0} \left(f_{n+1} + \rho_0 a_{n+1}\right) \cdot \eta dV_0 - \int_{\partial B_0} t_{n+1} \cdot \eta dS_0 = 0 \tag{7}$$

where P_{n+1} denotes the first Piola-Kirchoff stress field at time $t_{n+1,}$ and $f_{n+1}, a_{n+1}, t_{n+1}$ are the corresponding body forces, accelerations and boundary tractions respectively, ρ_0 is the mass density on the reference configuration, η is an admissible virtual displacement field and ∇V_0 denotes the material gradient. Upon discretization of the above equation, with finite elements, the governing equations become,

$$Ma_{n+1} + F^{\text{int}}_{n+1} = F^{ext}_{n+1} \tag{8}$$

where M is the lumped mass matrix, F^{ext} is the external force array including body forces and surface tractions and F^{int} is the internal force array arising from the current state of stress. The second order accurate central difference scheme is then used to discretize in time so that,

$$d_{n+1} = d_n + \Delta t v_n + \frac{1}{2}\Delta t^2 a_n \tag{9}$$

$$a_{n+1} = M^{-1}\left(F^{ext}_{n+1} - F^{\text{int}}_{n+1}\right) \tag{10}$$

$$v_{n+1} = v_n + \frac{1}{2}\Delta t\left(a_{n+1} + a_n\right) \tag{11}$$

where d, v and a denote the displacement, velocity and acceleration arrays respectively. Explicit integration is particularly convenient in impact problems, since the resolution of the various waves in the solution necessitates the use of small time steps well under the stability limit. In addition, explicit contact algorithms are more robust and simple than their implicit counterparts. This is a distinct advantage in problems involving fragmentation where complicated contact situations inevitably arise. Further, explicit integration is also advantageous in 3-dimensional calculations in terms of computational efficiency, as compared with implicit integration.

2.5. Geometry and meshing

Figure 1 shows the block and projectile system that was used in the simulation. The average grain size of an 87% alumina ceramic is 20 μm. The edge length of the cube was chosen as 4 mm so that the number of elements divided by the cube of edge length would roughly give an element size equivalent to the real grain size. The diameter of the ball was 0.4mm. A definitive contact surface was then generated giving due regard to the stress wave proliferation zones. The contact zone was about 3.5 mm^2. Infinite elements were used to form the opposite ends of the edge where the particle was supposed to interact with the material. This is in the sense that the material further away from the impact will not be affected by the interations. C3D8R type elements were used for the finite section and the corresponding CIN3D8 were used as infinite elements. Biasing was used while trying to regulate the mesh density so that the maximum number of elements were found in the vicinity of impact and less elements towards to infinite side of the block. A total of 134822 elements were used for the model, of which 7822 were resolved for the ball. Only one half of the ball was generated using symmetry. The ball was modelled using Solidworks while the block was generated in PATRAN 90. The block was held in the 1- and 3-axes while the ball was held in the 1-axis with translational and rotational degrees of freedom.

In 3-D modelling, the type of elements used did not permit the use of adaptive meshing. Consequently, the *FIXED MASS SCALING option was used to compensate for the computational efficiency involved in analysis of very small elements. The mass scaling option was used to scale the mass of the entire model on a per step basis. This was achieved by multiplying the masses of all elements by a constant scaling factor. During an impact analysis, elements near the impact zone typically experience large

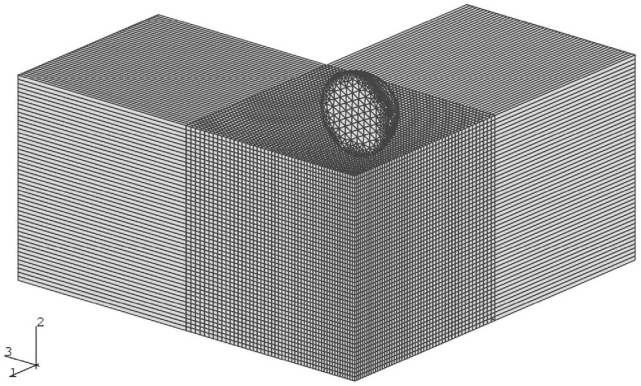

Fig. 1. Discretized FE model of block and ball

amounts of deformation. The reduced characteristic lengths of these elements results in a smaller global time increment. Scaling the mass of these elements throughout the the simulation can significantly reduce the computational time. Moreover, in cases where a moving body is impacting a stationary deformable body, increases in mass for these small elements during the simulations will have a negligible effect on the overall dynamic response. The particle possessed the basic material properties that of Garnet abrasive, a Young's modulus, E=248 GPa, Poisson's ratio, ν=0.3, a mass density, ρ=4120 kg/m^3. The block was assumed to possess material properties akin to 87% alumina ceramic, Young's modulus, E=221 GPa, Poisson's ratio, ν=0.22, a mass density, ρ=2410 kg/m^3.

3. Results

Figure 2 shows the von Mises stress configuration after impact at a velocity of 650 m/s. It is clear from the Mises stress profile that the stresses in the vicinity of impact are highly tensile and continue to emanate outward.

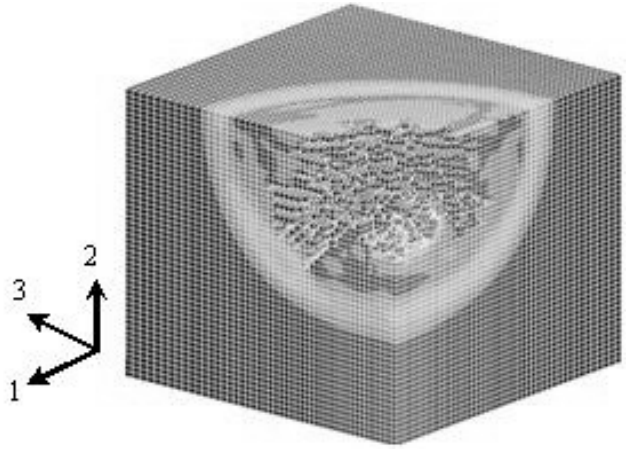

Fig. 2. Stress wave propagation in ceramics

The deformed mesh indicates that cracks are very isolated and restricted very much to the impact zone, although we have seen some element deletion using the failure criteria.. This seems valid in the sense that the fracture energy of these elements (grains) has crossed the nominal fracture energy per grain (and so, superceded the fracture toughness of that zone of material). This is confirmed by Figure 3 which shows the cracking stress profile at the impact siteClearly, the cracking stresses are maximum in that contact area (shown in deep red) than anywhere else. It should be pointed out that while the outer material is experiencing reasonably high cracking stresses, it appears that the elements (grains) in those regions are stable enough absorb energy that is much lesser than the nominal fracture energy.

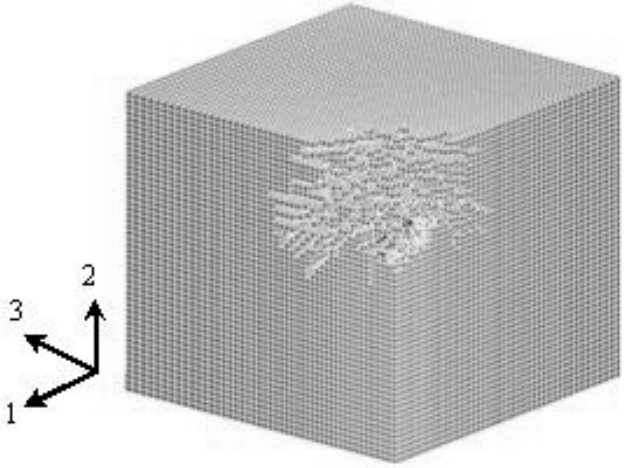

Fig. 3. Mixed mode cracking in brittle fracture of ceramics

3.1. Simulation of erosion mechanism using continuum zone dislocation

The simulations from the foregoing prompted to use ideal fracture conditions and optimal value of the coefficient of restitution (*e*). The particle was allowed to travel at a speed of 477 m/s, the average speed of a particle in an abrasive waterjet, with the aforementioned material properties. The strain rate was decreased here by an order of 10 so that the cracks were restricted to the continuum zone or rather contained in the continuum zone, thereby being removed after element deletion. In other words, it was assumed that the continuum behaved like a cohesive zone where all the elements reaching the threshold fracture energy values would be ready for element deletion. The results of the simulation were isolated and captured at four discrete time increments as shown in Figure 4 (a-d). At this stage, the number of elements dislocated from the mesh were calculated based on the maximum stress criteria. From the von Mises stress profiles, it can be seen that the pressure wave is followed by the stress wave and the progressive variation of the magnitude of these stresses (not shown due to space limitations) with progressive penetration of the particle.

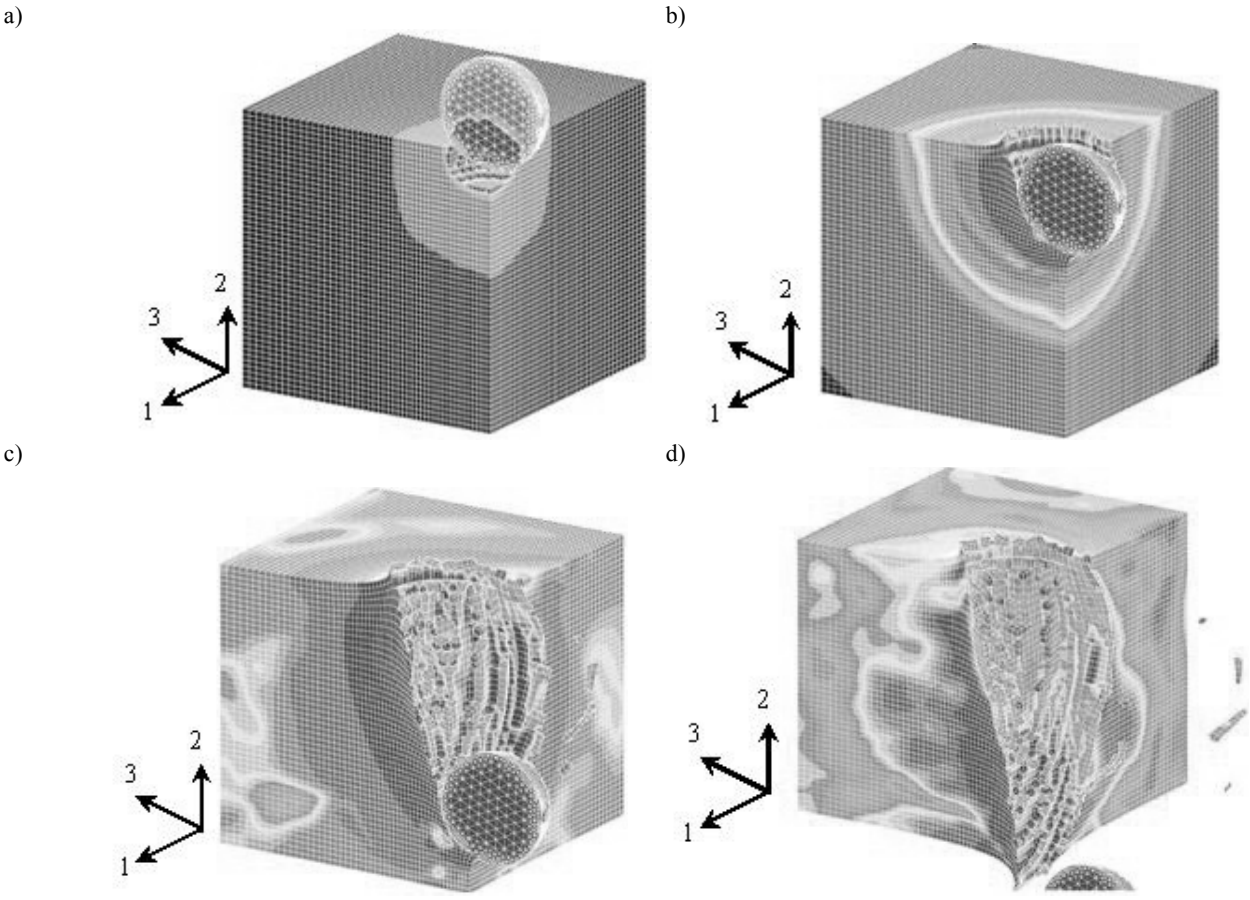

Fig. 4. Simulation of erosion process at 4 different instances

3.2. Comparison of erosion experiments with models

Figure 5 shows a comparison of the simulation results with our experimental results juxtaposed with those of Kim & Zeng's model. It can be seen that the model using the dynamic material properties predict lesser erosion rates for this class of alumina ceramics than the analytical model for a given impact speed.

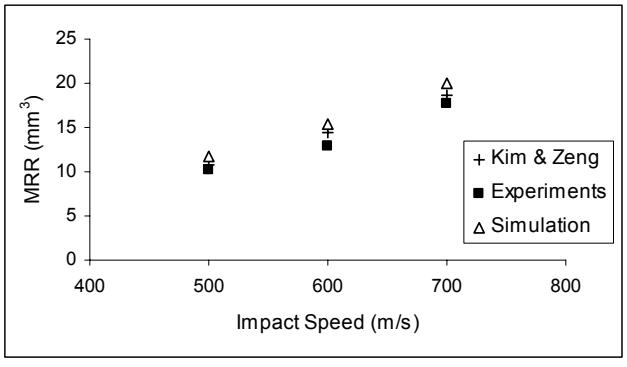

Fig. 5. Comparison of Material Removal Rates

3.3.Calculation of total volume of material removed per impact

In the FE model, the volume of each element is calculated by a simple procedure. The solid constituted 125000 elements over a length of 4 mm side of the cube. Let V_c be the total volume of the cube, and V_e the volume of each element. Then, $V_c = 4^3=64mm^3$ and $Ve = (64)/125000 = 5.12x10^{-4}$ mm^3. In a typical simulation shown in Figure 4, it is noted that 3566 elements have been removed from the mesh, giving an effective volume of elements as $V_e = (3566)(5.12x10^{-4}) = 0.018256$ mm^3. Kim & Zeng [12] give the following formula for the total volume of material removed per impact:

$$V = \frac{f_w \beta a \sigma_f m v^2 \sin^2 \alpha}{3\gamma E} + \frac{m v^2}{4\sigma_f} \times \left(\sin 2\alpha - 4\sin^2 \alpha + 38.12\nu \sin^3 \alpha \sqrt{\frac{\rho_p}{\sigma_f}} \right) \quad (12)$$

Using the various numerical values cited in their paper, we assume that the mean jet diameter is equal to 0.4 mm (as the averge orifice diameter can vary between 0.388 mm to 0.457 mm,

depending on the manufacturer). and proceed to calculate the total volume of material removed per impact as equal to 0.0163977 mm^3 for normal impact (α=0º).

Comparing the two values, we see that the percentage variation in the volume of material removed in the computer simulation using the finite element model varies is about 11.38%. The computational model provides us with a marginally higher erosion values as compared to the theoretical model. This is enterprising in the sense that we have stated with proof that a particle possessing such physical characteristics and properties is capable of removing such a quantity of material when it impacts a brittle material with selected properties, on the pre-condition that the coefficient of restitution holds, i.e. the particle does not rebound or shatter during the entire period of interaction with the material.

4. Conclusions

It can be seen that the model using the dynamic material properties predict higher erosion rates for this class of alumina ceramics than the theoretical model of Kim & Zeng [12]. One major drawback with their model is the use of a higher coefficient of restitution value of 0.2 as compared to our value of 0.1285. It is evident that for supersonic speeds, the value of *e* decreases, as explained by K.L Johnson [17]. This value can further be improved by assessing the porosity of the ceramics and other inherent subsurface flaws. We are not sure if this model can be scaled down to the actual particle size in the range of 300 μm and study the affects of volumetric material removed. However, we have shown that it is possible to venture down this path provided there is adequate computational power to run the models. The model can become very large as the size is reduced, as more and more number of elements would be required to discretisize the model.

References

[1] J.G.A Bitter, A study of erosion phenomena -Part 1, Wear 11 (1968) 5-21.

[2] F.P Bowden, J.E. Field,. The brittle fracture of solids by liquid, by solid and by shock, Proceedings of the Royal Society of London 282/1390 (1964) 331-352.

[3] F.W. Adler, Particulate impacts damage predictions, Wear 186-187 (1995) 35-44.

[4] M. Hashish, A model for abrasive waterjet (AWJ) machining, Journal of Engineering Materials and Technology 111 (1989) 154-162.

[5] J. Zeng,, T. Kim, A study of brittle mechanism applied to abrasive waterjet processes, Jet Cutting Technology, D. Saunders (Ed.), Elsevier, Amsterdam, 1991, 115-133

[6] A.G. Evans, M.E. Gulden, M. Rosenblatt, Impact damage in brittle materials in the elastic-plastic response regime, Proceedings of the Royal Society of London 361/1706 (1978) 343-365.

[7] P.A. Engel, Impacr Wear of Materials, Elsevier, Amsterdam, 1976.

[8] A.C. Evans, T.R. Wilshaw, Quasi-static solid particle damage in brittle solids- (i) Observations, analysis and implications, Acta Metallurgica 24 (1976) 939-956.

[9] A.K. Zurek, M.A. Meyers, Microstructural Aspects of Dynamic Failure, in High-Pressure Shock Compression of Solids II – Dynamic Fracture & Fragmentation, L. Davidson, D. E. Grady & M. Shahinpoor (Eds.), Springer-Verlag, 1996, 25-68.

[10] S.C. Hunter, Energy absorbed by elastic waves during impact, Journal of the Mechanics and Physics of Solids 5 (1957) 162-171.

[11] J. Zeng,, T. Kim, Material removal in polycrystalline ceramics by high pressure waterjet - an SEM study, International Journal of Waterjet Cutting Technology 1/2 (1991) 65-71.

[12] J. Zeng, J.T. Kim, An erosion model of polycrystalline ceramics in abrasive waterjet cutting, Wear 193 (1996) 207-217.

[13] I.M Hutchings, Energy absorbed by elastic waves during plastic impact, Journal of Physics 12 (1979) 1819-1824.

[14] D.R. Curran, L. Seaman Simplified Models of Fracture and Fragmentation, in High-Pressure Shock Compression of Solids II – Dynamic Fracture & Fragmentation, L. Davidson, D. E. Grady & M. Shahinpoor (Eds.), Springer-Verlag, 1996, 340-365.

[15] S.J Bless, A.M Rajendran, Initiation and Propagation of Damage Caused by Impact on Brittle Materials, in in High-Pressure Shock Compression of Solids II – Dynamic Fracture & Fragmentation, L. Davidson, D. E. Grady & M. Shahinpoor (Eds.), Springer-Verlag, 1996, 194-215.

[16] J.E. Ritter, P. Strzepa, K. Jakus, L. Rosenfeld, K.J. Buckman, Erosion damage in glass and alumina, Journal of the American Ceramic Society 67/11 (1984) 769-774.

[17] K.L Johnson, Contact Mechanics, Cambridge University Press, New York, 1987.